

# Helicity-dependent generalized parton distributions in constituent quark models

S. Boffi<sup>a</sup>, B. Pasquini<sup>a,b</sup>, M. Traini<sup>c</sup>

<sup>a</sup> Dipartimento di Fisica Nucleare e Teorica, Università degli Studi di Pavia  
and INFN, Sezione di Pavia, Pavia, Italy

<sup>b</sup> ECT\*, Villazzano (Trento), Italy

<sup>c</sup> Dipartimento di Fisica, Università degli Studi di Trento, Povo (Trento), and  
INFN, Gruppo Collegato di Trento, Trento, Italy

## Abstract

Helicity-dependent generalized parton distributions of the nucleon are derived from the overlap representation of generalized parton distributions using light-cone wave functions obtained in constituent quark models. Results from two different quark models are used also to study the angular momentum sum rule and the spin asymmetry in polarized electron scattering.

Key words: generalized parton distributions, constituent quark models  
PACS 12.39.-x, 13.60.Fz, 13.60.Hb, 14.20.Dh

## 1 Introduction

Over the years hard scattering processes in the deep inelastic scattering (DIS) regime have provided us with considerable insight into the internal nucleon structure, i.e. into its quark-gluon substructure as described by Quantum Chromodynamics (QCD). In particular, the spin-independent structure functions  $F_1(x)$ ,  $F_2(x)$ ,  $F_3(x)$  and the spin-dependent structure functions  $g_1(x)$ ,  $g_2(x)$  have been extracted as a function of the fraction  $x$  of the quark momentum along the direction of the fast moving nucleon (for a collection of data and fitting programmes, see Ref. [1]). As a consequence, it has been observed that the total nucleon momentum and spin are not exhausted by the quark contribution alone, and a large debate has originated on the involved quark-gluon dynamics (for a recent review, see Ref. [2]).

A significant step further in the investigation of such a dynamics is offered by the recently proposed generalized parton distributions (GPDs) [3, 4, 5, 6, 7, 8]. Their importance is due to the fact that they are candidate to give the most complete information on the internal nucleon dynamics and to provide us with a unifying theoretical background suitable to describe a variety of inclusive and

exclusive processes. GPDs are non-diagonal, off-forward hadronic matrix elements of bilocal products of the light-front quark and gluon field operators. As such they carry information on both the longitudinal and transverse distribution of partons in a fast moving nucleon and depend on  $x$ , the invariant momentum square  $t$ , and the so-called skewness parameter  $\xi$  describing the longitudinal change of the nucleon momentum. In total, both for quarks and gluons there are four distributions conserving the parton helicity and other four flipping it [9]. In the case of quarks, in the forward limit GPDs become diagonal matrix elements and three of them reduce to normal quark distributions, i.e. the momentum distribution  $q(x)$ , the helicity distribution  $\Delta q(x)$  and the transversity distribution  $\delta q(x)$ . Integrating the quark helicity conserving GPDs over  $x$  one obtains the nucleon electroweak form factors, that are given in terms of off-forward matrix elements of local operators as measured in exclusive reactions. The second moment of the unpolarized helicity conserving GPDs at  $t = 0$  gives a sum rule relating the total quark contribution (including quark orbital angular momentum) to the nucleon spin [5].

GPDs can be probed in deeply virtual Compton scattering (DVCS) and hard exclusive production of vector mesons (for recent reviews, see [10, 11, 12, 13, 14] and references therein). First data has become available [15] making the quest for modeling GPDs more urgent.

In the literature there are two approaches used to model the nucleon GPDs. One is a phenomenological construction based on reduction formulae where GPDs are related to the usual parton distributions by factorizing the momentum transfer dependence in agreement with the nucleon electroweak form factors [6, 16, 11, 17]. This leads to a parameterization of GPDs in terms of double distribution functions. However, this approximation is only expected to hold at relatively small values of  $-t$  [18]. In addition care must be taken to add the so-called D-term [19], an odd function having support  $|x| \leq |\xi|$  and required to satisfy the polynomiality property. This important property follows from Hermiticity and time-reversal, parity and Lorentz invariance and implies that the  $m$ -th moment in  $x$  of a GPD at  $t = 0$  is an even polynomial in  $\xi$  of degree less than or equal to  $m$  [10].

Another approach is based on direct calculation of GPDs in specific dynamical models. The first model calculations were performed using the MIT bag model [20]. The four helicity conserving GPDs were studied and shown to have a quite weak  $\xi$  dependence, while their  $t$  dependence roughly follows the nucleon form factors behaviour, thus confirming the intuition at the basis of the double-distribution assumption. However, the bag model breaks chiral symmetry by boundary conditions at the surface, and the initial and final nucleons are not good momentum eigenstates. As a consequence, a support violation occurs (with GPDs small, but nonvanishing beyond  $x = 1$ ) and the GPDs behaviour in the region  $|x| \leq |\xi|$  is not fully reliable. Moreover, an antiquark distribution with negative sign is produced when putting three valence quarks in the bag.

Further calculations have been performed in the chiral quark-soliton model [21, 18]. The model is based on an effective relativistic quantum field theory which was derived from the instanton model of QCD vacuum (see Ref. [22] and

references therein). The instanton fluctuations of the gluon field are simulated by a pion field binding the constituent quarks inside the nucleon. The model is theoretically justified in the limit of the large number of colours  $N_c$  and satisfies all general QCD requirements (sum rules, positivity, inequalities, etc.) including the polynomiality property [23]. However, the model comes with an intrinsic ultraviolet cutoff in the form of a momentum dependence of the constituent quark mass  $M(p)$ . The effects of the rapidly falling function  $M(p)$  are taken into account by using some regularization scheme. The uncertainty related to the details of the ultraviolet regularization leads to a 10–15% numerical uncertainty of the results [24]. In the limit of a large number of colours it describes a large variety of nucleonic properties typically within 30% accuracy [25, 12]. Concerning GPDs, in the leading order in the  $1/N_c$  expansion it is not possible to obtain results for separate flavours, only special flavour combinations being nonzero, i.e. the flavour singlet part of  $H(x, \xi, t)$  and the flavour isovector part of the unpolarized  $E(x, \xi, t)$  and of the helicity dependent GPDs,  $\tilde{H}(x, \xi, t)$  and  $\tilde{E}(x, \xi, t)$ .

A complete and exact overlap representation of GPDs has been recently worked out within the framework of light-cone quantization [26, 27]. In a preliminary investigation of such an approach presented in Ref. [28] a good description of parton distributions at large  $x$  has been achieved with a simple ansatz for the wave functions of the three lowest Fock states. In particular, for  $x \geq 0.6$  the 80% contribution is produced by the three valence quarks.

The same approach has been followed recently [29] investigating the link between light-cone wave functions (LCWFs) building the overlap representation of GPDs and wave functions derived in constituent quark models (CQMs). CQM wave functions can be considered as eigenfunctions of the nucleon Hamiltonian in the instant-form dynamics and can simply be related to wave functions in any form of relativistic Hamiltonian dynamics [30] according to the Bakamjian-Thomas construction [31]. Of course, this link is useful in the kinematic range where only (valence) quark degrees of freedom are effective. However, in this region GPDs are obtained in a covariant approach and exhibit the exact forward limit reproducing the parton distribution with the correct support and automatically fulfilling the particle number and momentum sum rule.

The method of Ref. [29] was applied to study quark helicity independent (unpolarized) GPDs. In this paper we extend it to quark helicity-dependent (polarized) GPDs completing the analysis of observable GPDs. In fact, both type occurs in DVCS, while hard meson electroproduction is sensitive to unpolarized or polarized GPDs depending on whether a longitudinal vector or a pseudoscalar meson is produced. In contrast, to date quark helicity flipping GPDs seem to contribute only in very peculiar selections of final states in two vector meson electroproduction [32].

The paper is organized as follows. In Section 2 the relevant definitions are summarized and the corresponding expressions in terms of the valence quark contribution are given in Section 3. The results obtained within two CQMs are presented in Section 4 where they are also applied to study nucleon spin asymmetries occurring in inclusive scattering of polarized electrons on polarized

targets. Concluding remarks are given in the final section and technical details are collected in the Appendix.

## 2 The helicity-dependent generalized parton distributions

We work in the so-called symmetric frame [26, 27]. The momentum of the initial (final) nucleon is  $P^\mu$  ( $P'^\mu$ ). The average nucleon momentum is then  $\bar{P}^\mu = \frac{1}{2}(P^\mu + P'^\mu)$ . The momentum transfer is given by  $\Delta^\mu = P'^\mu - P^\mu$ , the invariant momentum square is  $t = \Delta^2 = 2P \cdot \Delta$ , and the so-called skewness parameter is  $\xi = -\Delta^+ / 2\bar{P}^+$ . We also use the component notation  $a^\mu = [a^+, a^-, \vec{a}_\perp]$  for any four-vector  $a^\mu$  with light-cone components  $a^\pm = (a^0 \pm a^3)/\sqrt{2}$  and the transverse part  $\vec{a}_\perp = (a^1, a^2)$ .

The helicity-dependent GPDs are defined starting from the Fourier transform of the axial vector matrix element

$$\tilde{F}_{\lambda'\lambda}^q(\bar{x}, \xi, t) = \frac{1}{4\pi} \int dy^- e^{i\bar{x}\bar{P}^+ y^-} \langle P', \lambda' | \bar{\psi}(-\frac{1}{2}y) \not{n} \gamma^5 \psi(\frac{1}{2}y) | P, \lambda \rangle \Big|_{y^+ = \vec{y}_\perp = 0}, \quad (1)$$

where the four-vector  $n$  is a lightlike vector proportional to  $(1, 0, 0, -1)$ ,  $\lambda$  ( $\lambda'$ ) is the helicity of the initial (final) nucleon and the quark-quark correlation function is integrated along the light-cone distance  $y^-$  at equal light-cone time ( $y^+ = 0$ ) and at zero transverse separation ( $\vec{y}_\perp = 0$ ) between the quarks. The resulting one-dimensional Fourier integral along the light-cone distance  $y^-$  is with respect to the quark light-cone momentum  $\bar{k}^+ = \bar{x}\bar{P}^+$ . The link operator normally needed to make the definition (1) gauge invariant does not appear because we also choose the gauge  $A^+ = 0$  and assume that one can ignore the recently discussed transverse components of the gauge field [33, 34].

Following Ref. [5] the leading twist (twist-two) part of this amplitude can be parametrized as

$$\begin{aligned} \tilde{F}_{\lambda'\lambda}^q(\bar{x}, \xi, t) &= \frac{1}{2\bar{P}^+} \bar{u}(P', \lambda') \gamma^+ \gamma^5 u(P, \lambda) \tilde{H}^q(\bar{x}, \xi, t) \\ &\quad + \frac{1}{2\bar{P}^+} \bar{u}(P', \lambda') \frac{\Delta^+ \gamma^5}{2M} u(P, \lambda) \tilde{E}^q(\bar{x}, \xi, t), \end{aligned} \quad (2)$$

where  $u(P, \lambda)$  is the nucleon Dirac spinor and  $\tilde{H}^q(\bar{x}, \xi, t)$  and  $\tilde{E}^q(\bar{x}, \xi, t)$  are the helicity-dependent GPDs for partons of flavor  $q$ , corresponding on the nucleon side to an axial-vector and a pseudoscalar transition, respectively.

An explicit expression of the helicity-dependent GPDs in term of LCWF's has been obtained in Refs. [26, 27]. Having in mind the link between GPDs and CQM wave functions we will restrict our discussion into the region  $\xi < \bar{x} < 1$ .

In this region and in the symmetric frame

$$\begin{aligned} \tilde{F}_{\lambda'\lambda}^q(\bar{x}, \xi, t) = & \sum_{N,\beta} \left( \sqrt{1-\xi} \right)^{2-N} \left( \sqrt{1+\xi} \right)^{2-N} \sum_{j=1}^N \text{sign}(\mu_j) \delta_{s_j q} \\ & \times \int [d\bar{x}]_N [d\vec{k}_\perp]_N \delta(\bar{x} - \bar{x}_j) \Psi_{\lambda', N, \beta}^*(r') \Psi_{\lambda, N, \beta}(r) \Theta(\bar{x}_j), \end{aligned} \quad (3)$$

where  $s_j$  labels the quantum numbers of the  $j$ -th parton,  $\beta$  specifies all other quantum numbers necessary for the  $N$ -parton state, and  $\mu_j$  is the helicity of the active quark. The set of kinematical variables  $r, r'$  are defined as follows: for the final struck quark,

$$y'_j = \frac{\bar{k}_j^+ + \frac{1}{2}\Delta^+}{\bar{P}^+ + \frac{1}{2}\Delta^+} = \frac{\bar{x}_j - \xi}{1 - \xi}, \quad \vec{\kappa}'_{\perp j} = \vec{k}_{\perp j} + \frac{1}{2} \frac{1 - \bar{x}_j}{1 - \xi} \vec{\Delta}_\perp, \quad (4)$$

for the final  $N - 1$  spectators ( $i \neq j$ ),

$$y'_i = \frac{\bar{x}_i}{1 - \xi}, \quad \vec{\kappa}'_{\perp i} = \vec{k}_{\perp i} - \frac{1}{2} \frac{\bar{x}_i}{1 - \xi} \vec{\Delta}_\perp, \quad (5)$$

and for the initial struck quark

$$y_j = \frac{\bar{k}_j^+ - \frac{1}{2}\Delta^+}{\bar{P}^+ - \frac{1}{2}\Delta^+} = \frac{\bar{x}_j + \xi}{1 + \xi}, \quad \vec{\kappa}_{\perp j} = \vec{k}_{\perp j} - \frac{1}{2} \frac{1 - \bar{x}_j}{1 + \xi} \vec{\Delta}_\perp, \quad (6)$$

for the initial  $N - 1$  spectators ( $i \neq j$ ),

$$y_i = \frac{\bar{x}_i}{1 + \xi}, \quad \vec{\kappa}_{\perp i} = \vec{k}_{\perp i} + \frac{1}{2} \frac{\bar{x}_i}{1 + \xi} \vec{\Delta}_\perp. \quad (7)$$

Working out the spinor products we have

$$\begin{aligned} \tilde{F}_{++}^q(\bar{x}, \xi, t) &= -\tilde{F}_{--}^q(\bar{x}, \xi, t) \\ &= \sqrt{1 - \xi^2} \tilde{H}^q(\bar{x}, \xi, t) - \frac{\xi^2}{\sqrt{1 - \xi^2}} \tilde{E}^q(\bar{x}, \xi, t), \end{aligned} \quad (8)$$

$$\tilde{F}_{-+}^q(\bar{x}, \xi, t) = [F_{+-}^q(\bar{x}, \xi, t)]^* = \eta \xi \frac{\sqrt{t_0 - t}}{2M} \tilde{E}^q(\bar{x}, \xi, t), \quad (9)$$

where

$$\eta = \frac{\Delta^1 + i\Delta^2}{|\vec{\Delta}_\perp|}, \quad (10)$$

and

$$-t_0 = \frac{4\xi^2 M^2}{1 - \xi^2} \quad (11)$$

is the minimal value for  $-t$  at given  $\xi$ .

Using Eq. (2), one can derive  $\tilde{H}^q$  and  $\tilde{E}^q$  separately from the knowledge of  $\tilde{F}_{\lambda'\lambda}^q$ . In particular,  $\tilde{E}^q$  is directly given by Eq. (9), and

$$\tilde{H}^q(\bar{x}, \xi, t) = \frac{1}{\sqrt{1-\xi^2}} \left[ \tilde{F}_{++}^q(\bar{x}, \xi, t) + \frac{2M\xi}{\eta\sqrt{t_0-t}\sqrt{1-\xi^2}} \tilde{F}_{-+}^q(\bar{x}, \xi, t) \right]. \quad (12)$$

### 3 The valence-quark contribution

The valence-quark contribution to GPDs is obtained by specializing Eq. (3) to the case  $N = 3$ , i.e.

$$\begin{aligned} \tilde{F}_{\lambda'\lambda}^q(\bar{x}, \xi, t) &= \frac{1}{\sqrt{1-\xi^2}} \sum_{\lambda_i \tau_i} \sum_{j=1}^3 \delta_{s_j q} \text{sign}(\mu_j) \int [d\bar{x}]_3 [d\vec{k}_\perp]_3 \delta(\bar{x} - \bar{x}_j) \\ &\quad \times \Psi_{\lambda'}^{[f]*}(r', \{\lambda_i\}, \{\tau_i\}) \Psi_\lambda^{[f]}(r, \{\lambda_i\}, \{\tau_i\}) \Theta(\bar{x}_j), \end{aligned} \quad (13)$$

where  $\Psi_\lambda^{[f]}(r, \{\lambda_i\}, \{\tau_i\})$  is the eigenfunction of the light-front Hamiltonian of the nucleon, described as a system of three interacting quarks. It is here obtained from the corresponding solution  $\Psi_\lambda^{[c]}(\{\vec{k}_i\}, \{\lambda_i\}, \{\tau_i\})$  of the eigenvalue equation in the instant-form as described in Ref. [29]. Separating the spin-isospin component from the space part of the wave function,

$$\Psi_\lambda^{[c]}(\{\vec{k}_i\}, \{\lambda_i\}, \{\tau_i\}) = \psi(\vec{k}_1, \vec{k}_2, \vec{k}_3) \Phi_{\lambda\tau}(\lambda_1, \lambda_2, \lambda_3, \tau_1, \tau_2, \tau_3), \quad (14)$$

we have

$$\begin{aligned} \Psi_\lambda^{[f]}(r, \{\lambda_i\}, \{\tau_i\}) &= 2(2\pi)^3 \left[ \frac{1}{M_0} \frac{\omega_1 \omega_2 \omega_3}{\bar{x}_1 \bar{x}_2 \bar{x}_3} \right]^{1/2} \psi(\vec{k}_1, \vec{k}_2, \vec{k}_3) \\ &\quad \times \sum_{\mu_1 \mu_2 \mu_3} D_{\mu_1 \lambda_1}^{1/2*}(R_{cf}(\vec{k}_1)) D_{\mu_2 \lambda_2}^{1/2*}(R_{cf}(\vec{k}_2)) D_{\mu_3 \lambda_3}^{1/2*}(R_{cf}(\vec{k}_3)) \\ &\quad \times \Phi_{\lambda\tau}(\mu_1, \mu_2, \mu_3, \tau_1, \tau_2, \tau_3), \end{aligned} \quad (15)$$

where  $M_0$  is the mass of the non-interacting 3-quark system,  $\omega_i = (k_i^+ + k_i^-)/\sqrt{2}$ , and the Melosh rotations are given by

$$\begin{aligned} D_{\lambda\mu}^{1/2}(R_{cf}(\vec{k})) &= \langle \lambda | R_{cf}(\bar{x}M_0, \vec{k}_\perp) | \mu \rangle \\ &= \langle \lambda | \frac{m + \bar{x}M_0 - i\vec{\sigma} \cdot (\hat{z} \times \vec{k}_\perp)}{\sqrt{(m + \bar{x}M_0)^2 + \vec{k}_\perp^2}} | \mu \rangle. \end{aligned} \quad (16)$$

In the limit  $\Delta^\mu \rightarrow 0$ , where  $\bar{x}$  goes over to the parton momentum fraction  $x$ , we have

$$\tilde{H}^q(x, 0, 0) = \Delta q(x), \quad (17)$$

where  $\Delta q(x)$  is the polarized quark distribution of flavor  $q$ . Explicitly, the following simple expression is obtained

$$\begin{aligned} \Delta q(x) = & \sum_{\lambda_i \tau_i} \sum_{j=1}^3 \delta_{\tau_j \tau_q} \text{sign}(\mu_j) \\ & \times \int [d\vec{x}]_3 [d\vec{k}_\perp]_3 \delta(x - \bar{x}_j) |\Psi_\lambda^{[f]}(\{x_i\}, \{\vec{k}_{\perp,i}\}; \lambda_i, \tau_i)|^2. \end{aligned} \quad (18)$$

The polarized quark distribution  $\Delta q(x)$  combined with the unpolarized singlet quark distribution  $q(x) = H^q(x, 0, 0)$  and the unpolarized nonsinglet quark distribution  $E^q(x, 0, 0)$  determines the quark orbital-angular-momentum distribution  $L_q(x)$ , i.e. [35]

$$L_q(x) = \frac{1}{2} \{x[q(x) + e^q(x)] - \Delta q(x)\}, \quad (19)$$

where  $q(x) = H^q(x, 0, 0)$  and  $e^q(x) = E^q(x, 0, 0)$ . By integrating Eq. (19) over  $x$  one recovers the angular momentum sum rule [5]

$$J^q = \frac{1}{2} \int dx x [q(x) + e^q(x)] = \frac{1}{2} \Sigma^q + L^q, \quad (20)$$

where  $J^q$  is the fraction of the nucleon angular momentum carried by a quark of the flavour  $q$ , i.e. the sum of spin,

$$\frac{1}{2} \Sigma^q = \int dx \Delta q(x), \quad (21)$$

and orbital angular momentum,

$$L^q = \int dx L^q(x). \quad (22)$$

Thus, from the knowledge of  $\Delta q(x)$  and the unpolarized quark distributions one may infer the quark orbital angular momentum  $L^q$ .

Furthermore, by integrating the helicity-dependent GPDs over  $\bar{x}$ , for any value of the skewness  $\xi$ , one obtains the following relations

$$\int_{-1}^1 d\bar{x} \tilde{H}^q(\bar{x}, \xi, t) = G_A^q(t), \quad \int_{-1}^1 d\bar{x} \tilde{E}^q(\bar{x}, \xi, t) = G_P^q(t), \quad (23)$$

where  $G_A^q$  and  $G_P^q$  are the axial vector form factor and the induced pseudoscalar form factor of the quark of flavour  $q$ , respectively.

## 4 Results and discussion

In this Section we present results obtained within two constituent quark models, i.e. the relativistic version (HYP) [36] of the hypercentral quark model [37]

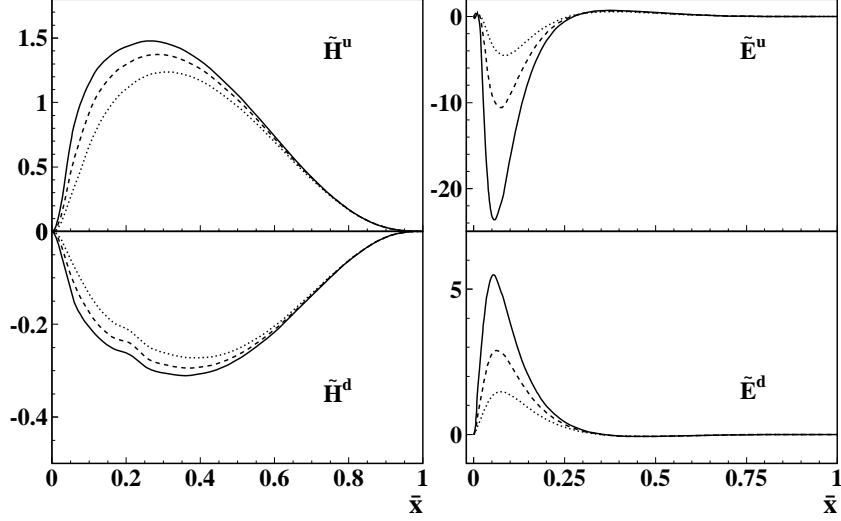


Figure 1: The helicity-dependent spin-averaged ( $\tilde{H}^q$ , left panels) and the helicity-flip ( $\tilde{E}^q$ , right panels) generalized parton distributions calculated in the GBE model for flavours  $u$  (upper panels) and  $d$  (lower panels), at  $\xi = 0$  and different values of  $t$ :  $t = 0$  (solid curves),  $t = -0.2 \text{ (GeV)}^2$  (dashed curves),  $t = -0.5 \text{ (GeV)}^2$  (dotted curves).

and the Goldstone-boson-exchange (GBE) model of Ref. [38]. In spite of its simplicity the hypercentral model is able to describe the basic features of the low-lying nucleon spectrum satisfactorily with a  $SU(6)$  symmetric nucleon wave function. With the GBE model the baryon spectrum is well reproduced up to 2 GeV with the correct orderings of the positive- and negative-parity states in the light and strange sectors. The resulting nucleon wave functions, without any further parameter, yield a remarkably consistent picture of the electroweak form factors within a point-form approach to quark dynamics [39].

Technical details concerning the derivation of the relevant formulae with these models are given in the Appendix.

The helicity-dependent GPDs calculated in the GBE model for the  $u$  and  $d$  flavours are plotted in Figs. 1–3 as a function of  $\bar{x}$  at different values of  $t$  and  $\xi$ . Both  $\tilde{H}^u$  and  $\tilde{H}^d$  exhibit a small  $t$ -dependence at  $\xi = 0$ . At constant  $t$ , their (rather weak)  $\xi$ -dependence is entirely governed by the requirement that  $\tilde{H}^q$  has to vanish at the boundaries of the allowed range  $\xi \leq \bar{x} \leq 1$  as a consequence of including only valence quarks in the present approach. Therefore the peak position of  $\tilde{H}^u$  and  $\tilde{H}^d$  for increasing  $\xi$  is shifted to higher values of  $\bar{x}$ . Due to the opposite sign of  $\tilde{H}^u$  and  $\tilde{H}^d$  in all kinematic conditions, their difference is positive and peaked at a value of  $\bar{x}$  comparable to the result obtained in the chiral quark-soliton model in the leading order of the  $1/N_c$  expansion [18]. Also  $\tilde{E}^u$  and  $\tilde{E}^d$  have opposite sign as functions of  $\bar{x}$ , their difference being rather small at intermediate and large values of  $\bar{x}$ . In fact, it is known that the



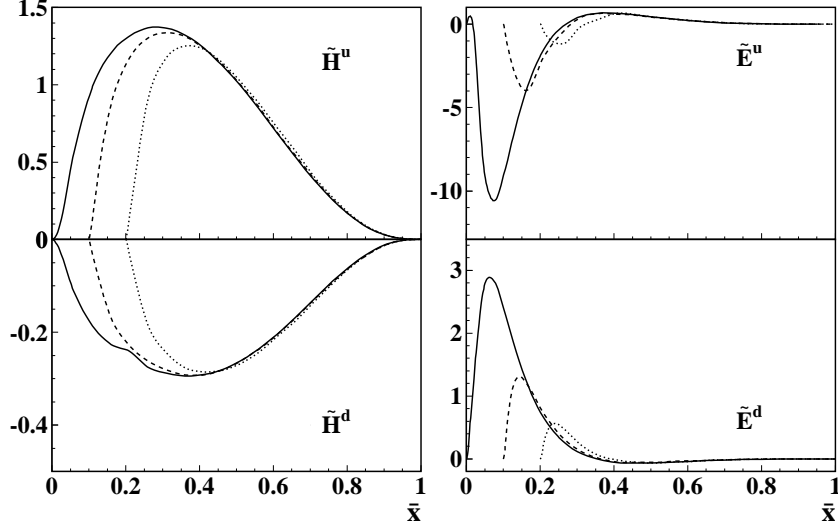


Figure 2: The same as in Fig. 1 but for fixed  $t = -0.2 \text{ (GeV)}^2$  and different values of  $\xi$ :  $\xi = 0$  (solid curves),  $\xi = 0.1$  (dashed curves),  $\xi = 0.2$  (dotted curves).

difference  $\tilde{E}^u - \tilde{E}^d$  is only significantly different from zero in the region  $|\bar{x}| \leq \xi$ , where it is dominated by the contribution of the pion pole [18].

The helicity-dependent GPDs calculated with the hypercentral and the GBE model behave quite similarly (Fig. 4) in spite of the fact that the hypercentral model is SU(6) symmetric, while the nucleon GBE wave function contains a small SU(6)-breaking part [38, 39]. However one should notice that the effect of SU(6) symmetry is not equivalent (for spin observables in particular) to the naive idea suggested by nonrelativistic dynamics. Within a relativistic approach the correlation between motion and spin (helicity) and the large content of high momentum components in the wavefunction (determined by the relativistic kinetic operator) change the intuitive picture considerably. In fact the SU(6)-breaking effects are emphasized (within a relativistic approach) by such correlations and high momentum tails, reducing the amount of explicit SU(6)-breaking terms required by nonrelativistic approaches. To better appreciate the symmetry effects on GPDs, it is worthwhile to discuss first the integral properties of diagonal spin and angular momentum observables as defined in Eqs. (20)–(22).

The different contributions entering the angular momentum sum rule (20) are presented in Table 1 as obtained in the nonrelativistic SU(6)-symmetric quark model, the hypercentral and the GBE model with the same valence quark distributions derived here and in our previous paper [29]. The differences between the nonrelativistic SU(6)-symmetric model and the hypercentral potential are entirely due to relativistic effects. In particular, the unpolarized nonsinglet quark distribution  $e^q(x) = E^q(x, 0, 0)$  vanishes in the nonrelativistic limit when all the valence quark are accommodated in the  $s$ -wave, while within the rela-

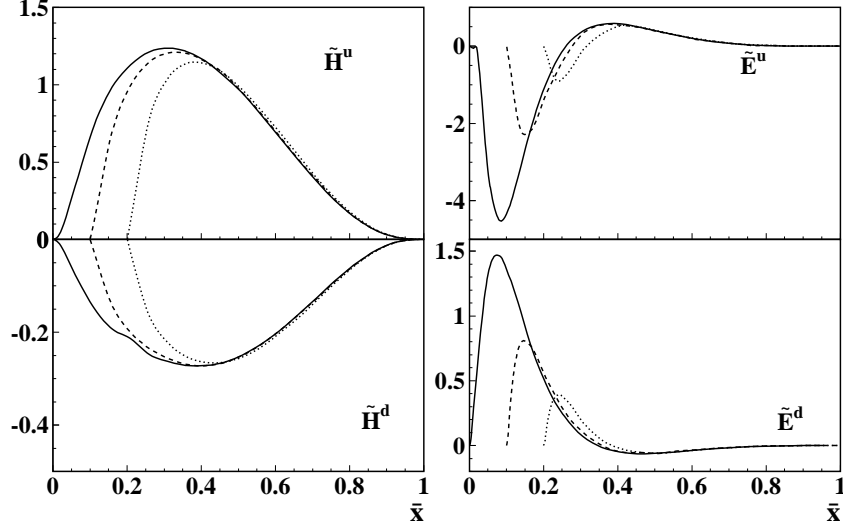


Figure 3: The same as in Fig. 1 but for fixed  $t = -0.5 \text{ (GeV)}^2$  and different values of  $\xi$ :  $\xi = 0$  (solid curves),  $\xi = 0.1$  (dashed curves),  $\xi = 0.2$  (dotted curves).

tivistic treatment the  $u$  and  $d$  contributions to  $e^q$  are quite sizeable in both the hypercentral and GBE models. It is remarkable that  $u$  quarks contribute much more than  $d$  quarks. This is expected and in agreement with previous findings from lattice QCD (see, e.g., Refs. [40, 41]). Only the small difference (0.27 in contrast to 0.20) can be ascribed to genuine SU(6)-breaking effects as considered by GBE. A similar behaviour can be found for the quark spin contributions ( $\Sigma^q$ ) and the (quark) angular momentum components ( $L^q$ ).

More specifically one can disentangle the effects due to Melosh rotations and the high momentum components including (as a “pedagogical” example) Melosh rotation into the calculations of spin observables performed with non-relativistic wavefunctions (which do not contain high momentum components). The effect is somehow surprising: the total quark spin part  $\Delta\Sigma$  (which reduces to 0.46 including  $u$  and  $d$  components in the HYP model) is enhanced up to 0.75 [42]. Let us remark that 0.75 (in contrast to the naive value 1.0 ascribed to nonrelativistic quark models) is often quoted as the “the relativistic reduction of quark spin contribution to the total nucleon spin due to lower components of the wave function”. Our results emphasize that the actual reduction is largely influenced by the consistent solution of the mass equation and a simplified guess could induce large uncertainties.

The integral properties shown in the Table 1 share, with all the results of the present paper, the limitation of considering valence contribution only. A consequence is the exact cancellation of the moments  $\int dx x e^u(x) + \int dx x e^d(x)$ . Indeed, the constraints of our model, i.e. no gluons, no sea and the momentum sum rule exhausted by valence quarks only, lead to  $\int dx x [e^u(x) + e^d(x)] = 0$ ,

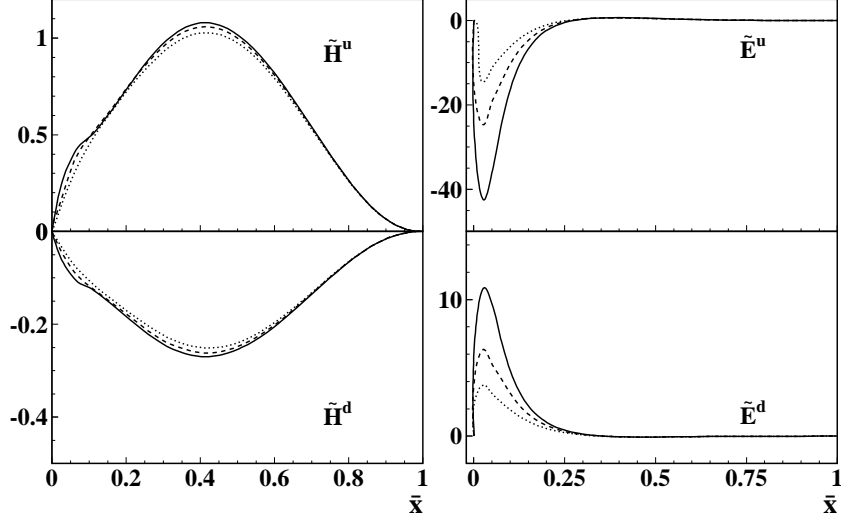


Figure 4: The same as in Fig. 1 but for the hypercentral model.

as shown in Table 1; a result, however, consistent with lattice QCD calculations [41].

In order to exploit all the potential features of the present approach and avoid the limitation mentioned, we perform a Leading Order evolution [43] (the only available evolution scheme established in the case of angular momentum densities) for the moments (20)–(22). One gets [36]

$$\begin{aligned}
\frac{1}{2}\Delta\Sigma(Q^2) &= \frac{1}{2}\Delta\Sigma(\mu^2); \\
L_q(Q^2) &= (b^{-50/81} - 1)\frac{1}{2}\Delta\Sigma(\mu^2) + b^{-50/81}L_q(\mu^2) - \frac{9}{50}(b^{-50/81} - 1); \\
J_g(Q^2) &= b^{-50/81}J_g(\mu^2) - \frac{8}{25}(b^{-50/81} - 1)
\end{aligned}$$

where  $b = \log(Q^2/\Lambda^2)/\log(\mu^2/\Lambda^2)$  and  $\mu^2 = 0.079 \text{ GeV}^2$  and  $\Lambda = 0.232 \text{ GeV}$ .

In the region  $Q^2 = 1 - 10 \text{ GeV}^2$ , the hypercentral (GBE) model predictions range from 0.04 to 0.014 (-0.03 to -0.06) for  $L_q$  and from 0.20 to 0.25 for  $J_g = L_g + \Delta g$  (and both potential models), results which are in good agreement with QCD sum rules predictions [44] ( $J_g \sim 0.25$ ) and lattice calculations [45] ( $J_g = 0.20 \pm 0.07$ ). Of course the predictions due to the nonrelativistic models behave quite differently, in particular one would expect  $L_q(Q^2) \sim -J_g \sim -0.25$  in the range  $Q^2 = 1 - 10 \text{ GeV}^2$  since  $\Delta\Sigma$  remains constant in  $Q^2$ . A detailed study [42] of the quark angular momentum distribution confirms such a behavior showing, in particular, a large difference of the results obtained within a relativistic and a nonrelativistic approach in the large- $x$  region. In addition it is important

Table 1: Valence contributions to the angular momentum sum rule calculated within the nonrelativistic SU(6)-symmetric quark model (NR-SU(6)), the SU(6)-symmetric hypercentral model (HYP) and the Goldstone-boson-exchange (GBE) model.

	NR-SU(6)	HYP	GBE
$\int dx x u(x)$	2/3	2/3	0.65
$\int dx x d(x)$	1/3	1/3	0.35
$\int dx x e^u(x)$	0	0.20	0.27
$\int dx x e^d(x)$	0	-0.20	-0.27
$\Sigma^u$	4/3	0.61	0.79
$\Sigma^d$	-1/3	-0.15	-0.18
$L^u$	0	0.13	0.065
$L^d$	0	0.14	0.13

to notice that our predictions obtained in the framework of vanishing gluon contribution,  $J_g(\mu^2) = 0$ , would not change much considering non vanishing  $J_g(\mu^2)$  models. As a matter of fact the scale  $\mu^2$  would rise (since at that scale the nonvanishing gluons would carry some momentum) and hence  $b$  would be larger for a given  $Q^2$ .

Concerning the second moment of GPDs, Eq. (23), we have the following axial and pseudoscalar coupling constants:  $g_A^{u,d} = G_A^{u,d}(0)$ ,  $g_P^{u,d} = (M_\mu/2M)G_P^{u,d}(t = -0.88M_\mu^2)$ , with  $M_\mu$  being the muon mass. The calculated values are given in Table 2 and are rather far from giving the experimental values. This is evidently due to neglecting higher Fock states in the present approach and, in the

Table 2: Axial and pseudoscalar coupling constants calculated with the hypercentral (HYP) and the Goldstone-boson-exchange (GBE) model.

	$g_A^u$	$g_A^d$	$g_P^u$	$g_P^d$
GBE	0.79	-0.18	-0.12	0.04
HYP	0.61	-0.15	-0.23	0.07

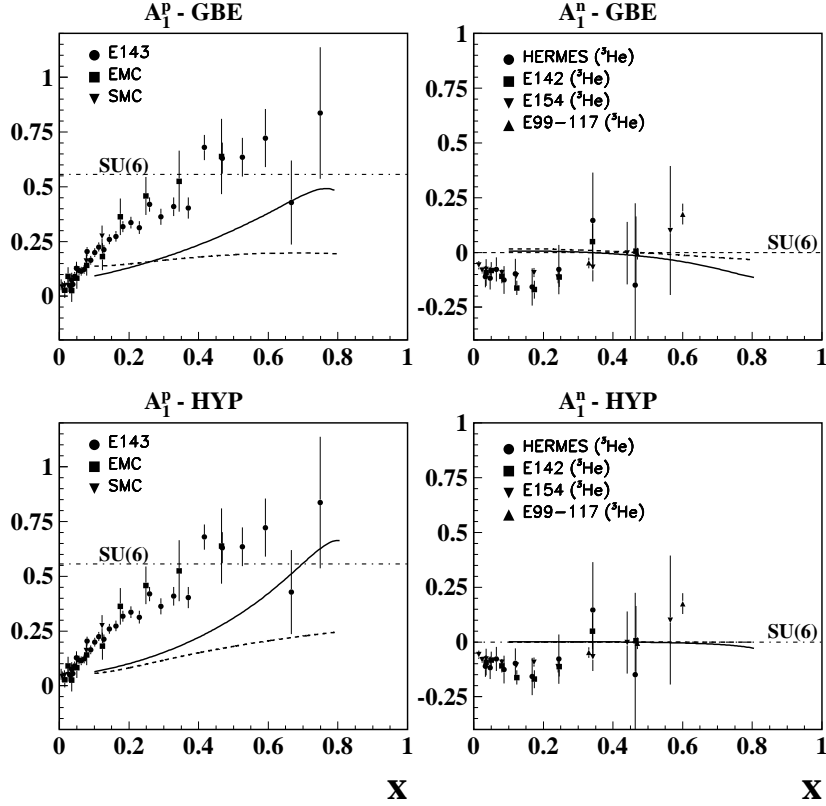


Figure 5: Proton ( $A_1^p$ , left panel) and neutron ( $A_1^n$ , right panel) spin asymmetries obtained with the GBE model (upper panels) and the hypercentral model (lower panels). Dashed curves refer to the hadronic scale  $\mu_0^2 \simeq 0.1 \text{ GeV}^2$ , solid curves are the result of the evolution at  $Q^2 = 3 \text{ GeV}^2$  up to NLO. Data from Refs. [47, 48, 49, 50] for the proton and from Refs. [51, 52, 53, 54, 55] for the neutron. The predicted SU(6) values are indicated by the dot-dashed line.

pseudoscalar case, to the missing pion-pole contribution dominating the low- $t$  part of the induced pseudoscalar form factor.

By studying the relativistic effects introduced by the light-front dynamics we stressed the similarities of the models we are considering, however one could also try to investigate better the role of the SU(6)-symmetry breaking introduced in the GBE model. To this end one can study the spin asymmetry  $A_1$ . Experimentally,  $A_1$  is extracted from the ratio of polarized cross sections in the deep inelastic regime as

$$A_1 = \frac{\sigma_{1/2} - \sigma_{3/2}}{\sigma_{1/2} + \sigma_{3/2}}, \quad (24)$$

where  $\sigma_{1/2(3/2)}$  is the total virtual photo-absorption cross section for the nucleon with a projection of 1/2 (3/2) for the total spin along the direction of the photon

momentum. At high  $Q^2$ ,  $A_1$  can be approximated as the ratio of the spin-dependent structure function  $g_1$  and the spin-independent structure function  $F_2$ . In addition, beyond  $x = 0.3$  where mainly valence quarks contribute,  $A_1$  for protons and neutrons, respectively, is given by

$$A_1^p(x) = \frac{4\Delta u(x) + \Delta d(x)}{4u(x) + d(x)}, \quad A_1^n(x) = \frac{\Delta u(x) + 4\Delta d(x)}{u(x) + 4d(x)}, \quad (25)$$

where  $u(x)$  ( $d(x)$ ) is the unpolarized and  $\Delta u(x)$  ( $\Delta d(x)$ ) the polarized quark distribution of flavour  $u$  ( $d$ ). In the SU(6) limit with both  $S = 0$  and  $S = 1$  diquark spin states equally contributing, one obtains  $A_1^p = 5/9$  and  $A_1^n = 0$ . However, at finite  $Q^2$  one has also to consider the  $Q^2$  dependence of quark distributions. This may introduce corrections to the SU(6) limit in spite of the fact that the spin asymmetry, being a ratio of distributions, should undergo a minimal  $Q^2$  dependence.

Assuming that the valence quark distributions derived from helicity-independent and helicity-dependent GPDs in the approach discussed here and in our previous paper [29] correspond to the hadronic scale  $\mu_0^2 \simeq 0.1 \text{ GeV}^2$ , close to the constituent quark mass,  $Q^2$  evolution is introduced along the lines of Ref. [46]. Results for  $A_1^p$  and  $A_1^n$  obtained with the GBE and the hypercentral model are shown in Fig. 5. In order to compare with available data the hadronic-scale results have been evolved to  $Q^2 = 3 \text{ GeV}^2$  at next-to-leading order (NLO). As a consequence of the contribution of sea quarks and gluons introduced by evolution, for larger  $x$  the results for the proton show an increasing trend shown also by data. In the neutron case within CQMs it is known that a relevant role is played by SU(6)-symmetry breaking [56]. Here, the very small SU(6)-breaking contribution turns out to be in the opposite direction with respect to recent measurements [55] that significantly indicates a positive  $A_1^n$  at  $x = 0.6$ . This discrepancy can ultimately be attributed to the behaviour of the unpolarized structure function  $F_2^n$  that increases with  $x$  (see also Ref. [57]). Let us stress, however, that the approach here described correctly incorporates the Pauli principle, a property crucial in understanding SU(6)-breaking effects (see Refs. [56, 57] for discussion).

## 5 Conclusions

The link between light-cone wave functions building the overlap representation of generalized parton distributions and wave functions derived in constituent quark models was introduced in Ref. [29] along the lines of Refs. [26, 27]. It has further been explored here by studying helicity-dependent generalized parton distributions of the nucleon. The approach, in principle correct in all kinematic regions, has an intrinsic limitation due to the use of the lowest order Fock-space components with three valence quark only. Results are therefore obtained in the range  $\xi \leq \bar{x} \leq 1$  and, when available, can be compared with data only in the kinematic range where valence quarks can be assumed as the relevant degrees

of freedom. However, they can be useful, e.g., in a  $Q^2$  evolution, and work in this direction is in progress.

Two quark models have been used, i.e. the relativistic hypercentral model of Ref. [36] and the Goldstone-boson-exchange model of Ref. [38]. The results are in qualitative agreement with the findings of the chiral quark-soliton model [18], a modest  $t$  dependence is found for  $\tilde{H}^q(\bar{x}, \xi, t)$  at  $\xi = 0$ , and the difference  $\tilde{E}^u(\bar{x}, \xi, t) - \tilde{E}^d(\bar{x}, \xi, t)$  is rather small in the valence region.

In an application to the spin asymmetry in polarized electron scattering the same trend of data is obtained for the proton, while the opposite sign at large  $x$  is found with respect to recent data on the neutron [55] in contrast with previous qualitative analyses based on CQMs with SU(6)-symmetry breaking [56]; a difference which can be explained by the correct inclusion of the Pauli principle in the present approach.

As a consequence of the correct relativistic link between wave functions of the constituent quark model and light-cone wave functions used in the overlap representation of generalized parton distributions, a significant contribution of valence quarks to the quark orbital angular momentum is found. This is a dynamical relativistic effect leading also to a nonvanishing  $E(\bar{x}, \xi, t)$  starting with only  $s$ -wave quarks, a result not obtainable in previous approaches directly based on light-cone wave functions.

## A Appendix

In this appendix we work out the summation over the spin and isospin variables appearing in the definition of the helicity amplitudes in Eq. (13). In the case of SU(6) symmetric CQM wave functions, the summation over isospin variables gives  $\delta_{T_{12}0} \delta_{\tau_3 1/2} + \delta_{T_{12}1} [\delta_{\tau_3 1/2} + 2\delta_{\tau_3 -1/2}]/3$  for the proton and  $\delta_{T_{12}0} \delta_{\tau_3 -1/2} + \delta_{T_{12}1} [2\delta_{\tau_3 1/2} + \delta_{\tau_3 -1/2}]/3$  for the neutron. On the other hand, the summation over the spin variables is carried out in a similar way as in Ref. [29] for the case of unpolarized GPDs, by using the explicit expressions of the Melosh-rotation matrices appearing in the initial and final light-cone wave function. As a result, Eq. (13) can be rewritten as

$$\begin{aligned} \tilde{F}_{\lambda'\lambda}^q &= \frac{3}{2} \frac{1}{\sqrt{1-\xi^2}} \frac{1}{(16\pi^3)^2} \int \prod_{i=1}^3 d\bar{x}_i \delta\left(1 - \sum_{i=1}^3 \bar{x}_i\right) \delta(\bar{x} - \bar{x}_3) \\ &\times \int \prod_{i=1}^3 d^2\vec{k}_{\perp,i} \delta\left(\sum_{i=1}^3 \vec{k}_{\perp,i}\right) \tilde{\psi}^*(\{y'_i\}, \{\vec{k}'_{\perp,i}\}) \tilde{\psi}(\{y_i\}, \{\vec{k}_{\perp,i}\}) \\ &\times \delta_{\tau_q \tau_3} \left\{ \tilde{X}_{\lambda'\lambda}^{00}(\vec{\kappa}', \vec{\kappa}) \delta_{\tau_3 1/2} + \frac{1}{3} \tilde{X}_{\lambda'\lambda}^{11}(\vec{\kappa}', \vec{\kappa}) [\delta_{\tau_3 1/2} + 2\delta_{\tau_3 -1/2}] \right\}, \quad (26) \end{aligned}$$

where

$$\tilde{\psi}(\{y_i\}, \{\vec{k}_{\perp,i}\}) = \left[ \frac{1}{M_0} \frac{\omega_1 \omega_2 \omega_3}{y_1 y_2 y_3} \right] \psi(\vec{\kappa}_1, \vec{\kappa}_2, \vec{\kappa}_3), \quad (27)$$

$$\begin{aligned}
\tilde{X}_{++}^{00}(\vec{\kappa}', \vec{\kappa}) &= -\tilde{X}_{--}^{00}(\vec{\kappa}', \vec{\kappa}) \\
&= \prod_{i=1}^3 N^{-1}(\vec{\kappa}'_i) N^{-1}(\vec{\kappa}_i) (A_1 A_2 + \vec{B}_1 \cdot \vec{B}_2) \tilde{A}_3, \quad (28)
\end{aligned}$$

$$\begin{aligned}
\tilde{X}_{++}^{11}(\vec{\kappa}', \vec{\kappa}) &= -\tilde{X}_{--}^{11}(\vec{\kappa}', \vec{\kappa}) = \prod_{i=1}^3 N^{-1}(\vec{\kappa}'_i) N^{-1}(\vec{\kappa}_i) \\
&\times \frac{1}{3} \left[ - (A_1 A_2 + \vec{B}_1 \cdot \vec{B}_2 - 4B_{1,z} B_{2,z}) \tilde{A}_3 \right. \\
&\quad + 2(A_1 B_{2,z} + A_2 B_{1,z}) \tilde{B}_{3,z} \\
&\quad + 2(B_{1,x} B_{2,z} + B_{1,z} B_{2,x}) \tilde{B}_{3,y} \\
&\quad \left. + 2(B_{1,y} B_{2,z} + B_{1,z} B_{2,y}) \tilde{B}_{3,x} \right], \quad (29)
\end{aligned}$$

$$\begin{aligned}
\text{Re} \left( \tilde{X}_{-+}^{00}(\vec{\kappa}', \vec{\kappa}) \right) &= \text{Re} \left( \tilde{X}_{+-}^{00}(\vec{\kappa}', \vec{\kappa}) \right) \\
&= \prod_{i=1}^3 N^{-1}(\vec{\kappa}'_i) N^{-1}(\vec{\kappa}_i) \left[ (A_1 A_2 + \vec{B}_1 \cdot \vec{B}_2) \tilde{B}_{3,y} \right], \quad (30)
\end{aligned}$$

$$\begin{aligned}
\text{Im} \left( \tilde{X}_{-+}^{00}(\vec{\kappa}', \vec{\kappa}) \right) &= -\text{Im} \left( \tilde{X}_{+-}^{00}(\vec{\kappa}', \vec{\kappa}) \right) \\
&= \prod_{i=1}^3 N^{-1}(\vec{\kappa}'_i) N^{-1}(\vec{\kappa}_i) \left[ (A_1 A_2 + \vec{B}_1 \cdot \vec{B}_2) \tilde{B}_{3,x} \right], \quad (31)
\end{aligned}$$

$$\begin{aligned}
\text{Re} \left( \tilde{X}_{-+}^{11}(\vec{\kappa}', \vec{\kappa}) \right) &= \text{Re} \left( \tilde{X}_{+-}^{11}(\vec{\kappa}', \vec{\kappa}) \right) = \prod_{i=1}^3 N^{-1}(\vec{\kappa}'_i) N^{-1}(\vec{\kappa}_i) \\
&\times \frac{1}{3} \left[ (-A_1 A_2 - \vec{B}_1 \cdot \vec{B}_2 + 4B_{1,x} B_{2,x}) \tilde{B}_{3,y} \right. \\
&\quad + 2(A_1 B_{2,x} + A_2 B_{1,x}) \tilde{B}_{3,z} \\
&\quad + 2(B_{1,x} B_{2,z} + B_{1,z} B_{2,x}) \tilde{A}_3 \\
&\quad \left. + 2(B_{1,x} B_{2,y} + B_{1,y} B_{2,x}) \tilde{B}_{3,x} \right], \quad (32)
\end{aligned}$$

$$\begin{aligned}
\text{Im} \left( \tilde{X}_{-+}^{11}(\vec{\kappa}', \vec{\kappa}) \right) &= -\text{Im} \left( \tilde{X}_{+-}^{11}(\vec{\kappa}', \vec{\kappa}) \right) = \prod_{i=1}^3 N^{-1}(\vec{\kappa}'_i) N^{-1}(\vec{\kappa}_i) \\
&\times \frac{1}{3} \left[ (-A_1 A_2 - \vec{B}_1 \cdot \vec{B}_2 + 4B_{1,y} B_{2,y}) \tilde{B}_{3,x} \right. \\
&\quad + 2(A_1 B_{2,y} + A_2 B_{1,y}) \tilde{B}_{3,z} \\
&\quad + 2(B_{1,x} B_{2,y} + B_{1,y} B_{2,x}) \tilde{B}_{3,y} \\
&\quad \left. + 2(B_{1,y} B_{2,z} + B_{1,z} B_{2,y}) \tilde{A}_3 \right]. \quad (33)
\end{aligned}$$

In the above equations,  $N(\vec{\kappa})$ ,  $A_i$  and  $\vec{B}_i$ , with  $i = 1, 2$ , are defined as in Ref. [29] and reported here for convenience

$$N(\vec{\kappa}) = [(m + yM_0)^2 + \vec{\kappa}_\perp^2]^{1/2}. \quad (34)$$



$$A_i = (m + y'_i M'_0)(m + y_i M_0) + \kappa'_{i,y} \kappa_{i,y} + \kappa'_{i,x} \kappa_{i,x}, \quad (35)$$

$$B_{i,x} = -(m + y'_i M'_0) \kappa_{i,y} + (m + y_i M_0) \kappa'_{i,y}, \quad (36)$$

$$B_{i,y} = (m + y'_i M'_0) \kappa_{i,x} - (m + y_i M_0) \kappa'_{i,x}, \quad (37)$$

$$B_{i,z} = \kappa'_{i,x} \kappa_{i,y} - \kappa'_{i,y} \kappa_{i,x}, \quad (38)$$

while  $\tilde{A}_3$  and  $\vec{\tilde{B}}_3$  are given by

$$\tilde{A}_3 = (m + y'_3 M'_0)(m + y_3 M_0) - \kappa'_{3,y} \kappa_{3,y} - \kappa'_{3,x} \kappa_{3,x}, \quad (39)$$

$$\tilde{B}_{3,x} = (m + y'_3 M'_0) \kappa_{3,y} + (m + y_3 M_0) \kappa'_{3,y}, \quad (40)$$

$$\tilde{B}_{3,y} = (m + y'_3 M'_0) \kappa_{3,x} + (m + y_3 M_0) \kappa'_{3,x}, \quad (41)$$

$$\tilde{B}_{3,z} = \kappa'_{3,x} \kappa_{3,y} - \kappa'_{3,y} \kappa_{3,x}, \quad (42)$$

with  $y_i$ ,  $y'_i$ , and  $\kappa_i$ ,  $\kappa'_i$ , for  $i = 1, 2, 3$ , defined in Eqs. (4) - (7).

In the GBE model the nucleon wave functions are expanded on a basis where the spin-isospin part is combined with a space part in the form of correlated Gaussian functions of the Jacobi coordinates referring to a particular partition. The total wave function is a symmetrized linear combination of such basis functions over the three possible partitions thus ultimately violating SU(6) symmetry. The calculation with the GBE wave function requires repeating the same steps as with the hypercentral wave functions for each partition of the partial contribution to the total initial (final) nucleon wave function.

## References

- [1] Durham HEP Database Group, <http://durpdg.dur.ac.uk/HEPDATA>.
- [2] B.W. Filippone and X. Ji, Adv. Nucl. Phys. 26 (2001) 1.
- [3] D. Müller, D. Robaschik, B. Geyer, F.M. Dittes, J. Hořejši, Fortsch. Phys. 42 (1994) 101.
- [4] A.V. Radyushkin, Phys. Lett. B 380 (1996) 417; Phys. Lett. B 385 (1996) 333.
- [5] Xiangdong Ji, Phys. Rev. Lett. 78 (1997) 610.
- [6] A.V. Radyushkin, Phys. Rev. D 56 (1997) 5524.
- [7] Xiangdong Ji, Phys. Rev. D 55 (1997) 7114.
- [8] J.C. Collins, L.L. Frankfurt and M. Strikman, D 56 (1997) 2982.
- [9] M. Diehl, Eur. Phys. J. C 19 (2001) 485.
- [10] Xiangdong Ji, J. Phys. G 24 (1998) 1181.

- [11] A.V. Radyushkin, in *At the Frontier of Particle Physics*, Vol. 2, edited by M. Shifman (World Scientific, Singapore, 2001), p. 1037, hep-ph/0101225.
- [12] K. Goeke, M.V. Polyakov and M. Vanderhaeghen, *Progr. Part. Nucl. Phys.* 47 (2001) 401.
- [13] M. Vanderhaeghen, *Nucl. Phys. A* 711 (2002) 109.
- [14] M. Diehl, hep-ph/0307382.
- [15] HERMES Collaboration, A. Airapetian *et al.*, *Phys. Rev. Lett.* 87 (2001) 182001; CLAS Collaboration, S. Stepanyan *et al.*, *Phys. Rev. Lett.* 87 (2001) 182002; H1 Collaboration, C. Adloff *et al.*, *Phys. Lett. B* 517 (2001) 47.
- [16] A.V. Radyushkin, *Phys. Rev. D* 59 (1999) 014030; *Phys. Lett. B* 449 (1999) 81.
- [17] M. Vanderhaeghen, P.A.M. Guichon and M. Guidal, *Phys. Rev. D* 60 (1999) 094017.
- [18] M. Penttinen, M.V. Polyakov and K. Goeke, *Phys. Rev. D* 62 (2000) 014024.
- [19] M.V. Polyakov and C. Weiss, *Phys. Rev. D* 60 (1999) 114017.
- [20] X. Ji, W. Melnitchouk and X. Song, *Phys. Rev. D* 56 (1997) 5511.
- [21] V.Yu. Petrov, P.V. Pobylitsa, M.V. Polyakov, I. Börnig, K. Goeke and C. Weiss, *Phys. Rev. D* 57 (1998) 4325.
- [22] D.I. Diakonov, V.Yu. Petrov, P.V. Pobylitsa, *Nucl. Phys. B* 306 (1988) 809.
- [23] P. Schweitzer, S. Boffi, M. Radici, *Phys. Rev. D* 66 (2002) 114004; *Nucl. Phys. A* 711 (2002) 207; P. Schweitzer, M. Colli, S. Boffi, *Phys. Rev. D* 67 (2003) 114022.
- [24] D.I. Diakonov, V.Yu. Petrov, P.V. Pobylitsa, M.V. Polyakov, C. Weiss, *Phys. Rev. D* 58 (1998) 038502.
- [25] Ch. Christov *et al.*, *Progr. Part. Nucl. Phys.* 37 (1996) 91.
- [26] M. Diehl, Th. Feldmann, R. Jakob and P. Kroll, *Nucl. Phys. B* 596 (2001) 33.
- [27] S.J. Brodsky, M. Diehl and D.S. Hwang, *Nucl. Phys. B* 596 (2001) 99.
- [28] M. Diehl Th. Feldmann, P. Kroll and R. Jakob, *Eur. Phys. J. C* 8 (1999) 409.
- [29] S. Boffi, B. Pasquini and M. Traini, *Nucl. Phys. B* 649 (2003) 243.
- [30] B.D. Keister and W.N. Polyzou, *Adv. Nucl. Phys.* 20 (1991) 225.

- [31] B. Bakamjian and L.H. Thomas, Phys. Rev. 92 (1953) 1300.
- [32] D.Yu. Ivanov, B. Pire, L. Szymanowski and O.V. Teryaev, Phys. Lett. B 550 (2002) 65.
- [33] S.L. Brodsky, P. Hoyer, N. Marchal, S. Peigné, F. Sannino, Phys. Rev. D 65 (2002) 114025.
- [34] A.V. Belitsky, X. Ji, F. Yuan, Nucl. Phys. B 656 (2003) 165.
- [35] P. Hoodbhoy, Xiangdong Ji and Wei Lu, Phys. Rev. D 59 (1999) 014013.
- [36] P. Faccioli, M. Traini and V. Vento, Nucl. Phys. A 656 (1999) 400.
- [37] M. Ferraris, M.M. Giannini, M. Pizzo, E. Santopinto, L. Tiator, Phys. Lett. B 364 (1995) 231.
- [38] L.Ya. Glozman, W. Plessas, K. Varga and R.F. Wagenbrunn, Phys. Rev. D 58 (1998) 094030.
- [39] R.F. Wagenbrunn, S. Boffi, W. Klink, W. Plessas and M. Radici, Phys. Lett. B 511 (2001) 33; L.Ya. Glozman, M. Radici, R.F. Wagenbrunn, S. Boffi and W. Plessas, Phys. Lett. B 516 (2001) 183; S. Boffi, L.Ya. Glozman, W. Klink, W. Plessas, M. Radici and R.F. Wagenbrunn, Eur. Phys. J. A 14 (2002) 17.
- [40] M. Göckeler *et al.* (QCDSF Collaboration), hep-ph/0304249.
- [41] Ph. Hägler, T.W. Negele, D.B. Renner and W. Schroers, Phys. Rev. D 68 (2003) 034505.
- [42] F. Cano, P. Faccioli, S. Scopetta and M. Traini, Phys. Rev. D 62 (2000) 054023.
- [43] O. Martin, P. Hägler and A. Schäfer, Phys. Lett. B 448 (1999) 99.
- [44] I.I. Balitsky and X. Ji, Phys. Rev. Lett. 79 (1997) 1225.
- [45] N. Mathur, S.J. Dong, K.F. Liu, L. Mankiewicz and N. Mukhopadhyay, Phys. Rev. D 62 (2000) 114504.
- [46] M. Traini, V. Vento, A. Mair and A. Zambarda, Nucl. Phys. A 614 (1997) 472; A. Mair and M. Traini, Nucl. Phys. A 624 (1997) 564; A 628 (1998) 296.
- [47] E143 Collaboration, K. Abe *et al.*, Phys. Rev. D 58 (1998) 112003.
- [48] E155 Collaboration, P.L. Anthony *et al.*, Phys. Lett. B 493 (2000) 19.
- [49] EMC Collaboration, J. Ashman *et al.*, Phys. Lett. B 206 (1988) 364; Nucl. Phys. B 328 (1989) 1.

- [50] SMC Collaboration, B. Adeva *et al.*, Phys. Rev. D 60 (1999) 072004.
- [51] E142 Collaboration, P.L. Anthony *et al.*, Phys. Rev. D 54 (1996) 6620.
- [52] E154 Collaboration, K. Abe *et al.*, Phys. Lett. B 405 (1997) 180; Phys. Rev. Lett. 79 (1997) 26.
- [53] SMC Collaboration, D. Adams *et al.*, Phys. Lett. B 357 (1995) 248.
- [54] HERMES Collaboration, K. Ackerstaff *et al.*, Phys. Lett. B 404 (1997) 383; HERMES Collaboration, A. Airapetian *et al.*, Phys. Lett. B 442 (1998) 484.
- [55] X. Zheng, Ph. D. Thesis, M.I.T., 2002; Jlab Collaboration (E99-117) X. Zheng *et al.*, to be published.
- [56] N. Isgur, Phys. Rev. D 59 (1999) 034013.
- [57] B. Pasquini, M. Traini and S. Boffi, Phys. Rev. D 65 (2002) 074028.